

## Molecular Crowding and Protein Diffusion in Biological Membranes

**Key Words:** *self-diffusion, protein-protein interactions, Saffman-Delbrück equation, fluorescence recovery after photobleaching, lattice-gas model, free-volume model, Brownian theory*

### 1. INTRODUCTION

It is by now apparent that biological membranes are far from static, ideal mixtures of their protein and lipid components. Nowhere is this fact more strikingly manifest than in the complex diffusive behavior of membrane proteins. For example, not only are membrane proteins typically mobile, their mobility is influenced by many variables. These include protein size, protein concentration, and the lipid composition of the membrane,<sup>1-3</sup> as well as binding to the cytoskeletal or extracellular matrices and confinement to domains by the cytoskeleton and tight junctions.<sup>4-7</sup>

Theoretical work can help to unravel the complexities of membrane protein diffusion. For example, shortly after the introduction of the Fluid Mosaic model,<sup>8</sup> Saffman and Delbrück were able to derive an equation<sup>9</sup> that has proven very successful at describing protein diffusion in simple, dilute, reconstituted membranes. This equation has proven less successful, however, at describing diffusion in biological membranes, where protein concentrations are

high and proteins interact with their neighbors. Recent theoretical work has therefore focused on an analysis of these more complicated systems, in which interprotein interactions affect protein motion.

In this article we summarize recent theoretical studies of the *self*-diffusion of interacting membrane proteins. The system under consideration will be relatively simple: a single-phase membrane containing lipid and one species of protein present at high concentration. It is our belief that an analysis of the relationship between interactions and protein diffusion in such a simple system provides a foundation upon which to formulate descriptions of protein mobility in complex biological membranes. Our discussion begins with a definition of self-diffusion and a description of theoretical analyses that are applicable only at infinite protein dilution. We then describe models of the self-diffusion of interacting membrane proteins. We conclude by comparing the theoretical predictions with experimental data. In the Appendix, we consider, briefly, extensions of the theoretical models to systems containing immobile proteins and multiple species of proteins.

## 2. DEFINITION OF SELF-DIFFUSION

Here self-diffusion is taken to refer to the random, translational motion of *individual* protein molecules.\* Such motion has its origin in collisions between a protein and other molecules in and around the fluid bilayer. Though random, this diffusive motion has certain statistical properties that can be described mathematically using a self-diffusion coefficient,  $D^s$ . For example, the mean-square displacement,  $\langle r^2 \rangle$ , of proteins and the time,  $t$ , are related by the equation†

$$\langle r^2(t) \rangle = 4D^s t. \quad (1)$$

Theories of self-diffusion seek to derive expressions for this diffusion coefficient valid under the conditions of interest.

## 3. THEORIES OF DIFFUSION AT INFINITE PROTEIN DILUTION‡

At infinite protein dilution, protein motion is determined by random, Brownian collisions with lipid and the aqueous media bounding the membrane. The diffusion coefficient describing this simplest theoretical case was first obtained by Saffman and Delbrück,<sup>9,10</sup> using the model in Fig. 1a. Their work was later generalized to describe systems with arbitrary extramembranous viscosity<sup>11</sup> and porous protein aggregates.<sup>12</sup> We do not repeat these theoretical developments, but instead note that for a single protein, the diffusion coefficient may be written

$$D_0 = (k_B T / 4\pi\eta_m h) [\log(2/\epsilon) - \gamma + (4/\pi)\epsilon - (\epsilon^2/2)\log(2/\epsilon)], \quad (2a)$$

$$\epsilon = (a/h)[(\eta_1 + \eta_2)/\eta_m], \quad (2b)$$

where  $k_B$  is Boltzmann's constant,  $T$  is the temperature,  $\eta_m$  is the viscosity of the membrane,  $h$  is the thickness of the membrane,  $\gamma$  is Euler's constant (0.5772),  $a$  is the radius of the protein, and  $\eta_1$  and  $\eta_2$  are the viscosities of the fluid on opposite sides of the membrane.<sup>11</sup> The subscript zero on  $D_0$  is meant to serve as a reminder that this diffusion coefficient describes motion in a dilute solution (nominally at "zero" concentration). Equation (2) has been carefully tested and found to hold quite well at low protein concentrations.<sup>1-3</sup> For further discussion of protein diffusion at infinite dilution we refer the reader to more detailed reviews.<sup>1-3</sup>

## 4. THEORIES OF SELF-DIFFUSION AT FINITE PROTEIN CONCENTRATIONS

At finite protein concentrations, protein diffusion is affected by interprotein interactions, as well as interactions with lipids and the aqueous media. Simple excluded-volume interactions, which arise because two molecules cannot simultaneously occupy the same

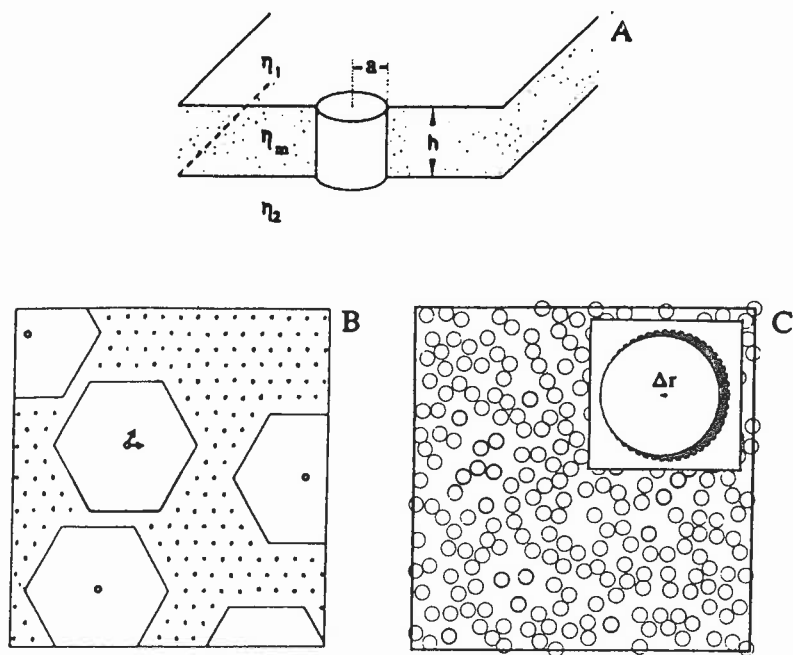


FIGURE 1 Pictures of models. (A) Saffman–Delbrück model. The symbols are defined in the text following Eq. (2). After Ref. 2. (B) Lattice-gas model. Here hexagonal proteins are shown on a triangular lattice. The arrows indicate the two directions (of a possible six) that the protein can move without colliding with a neighbor. From Ref. 13. (C) Free-volume and Brownian models. Protein coordinates were generated by continuum Monte Carlo simulation and used to generate the probability distributions that appear in the Brownian model. Spaces between particles can be taken to represent “free volumes.” The inset defines the target area used in the free-volume calculations and the quantity  $\Delta r$ , which determines the free parameter  $x \equiv \Delta r/a$  appearing in Eq. (6). After Refs. 35 and 82. Note that only the Saffman–Delbrück model explicitly takes into account the three-dimensional character of the membrane. All of the theories of interaction-dependent diffusion model a two-dimensional projection of protein motion; thus, the pictures in Panels (B) and (C) represent views along the membrane normal. The validity of purely two-dimensional treatments of interaction-dependent diffusion has been discussed (Refs. 43 and 70).

space, and long-range electrostatic and lipid-mediated interactions are examples of protein–protein forces that influence diffusion at high protein concentrations. The somewhat less familiar hydrodynamic interaction (defined below) could also affect dynamics in membranes. At finite protein concentrations, Eq. (2) no longer

holds. However, it is still possible to define a protein diffusion coefficient that satisfies Eq. (1). In this section we describe three theoretical approaches used to derive this diffusion coefficient—lattice-gas models, free-volume models, and Brownian models—and explore their predictions. Please note that the reference state for these models corresponds to infinite protein dilution; results are, therefore, summarized as a ratio  $D^*/D_0$ .

#### 4.1. Lattice Gas Models

*4.1.1. Description of theory.* Modeling diffusion in a concentrated biological membrane is a considerable theoretical challenge because many-particle dynamics is complex. A standard theoretical goal is to construct an analytical model of the problem of interest; however, in the lattice-gas approach the difficulties inherent in constructing such a description are overcome instead by numerically simulating diffusion.<sup>13–19</sup> Further simplifications restrict proteins to a lattice and typically confine interactions to nearest neighbors, though long-range potentials can also be studied<sup>14,18,19</sup> (see Fig. 1b). The lattice-gas models of membrane protein diffusion build upon the detailed description of lattice gases found in the physics literature.<sup>20–22</sup>

Simulations of protein motion are performed according to standard lattice Monte Carlo algorithms.<sup>23</sup> Initially, proteins are distributed randomly on a regular “polyhedryl” lattice at a desired concentration. Both the geometry of the lattice and the size of the proteins relative to the lattice spacing are taken as variables. The boundaries of the lattice are treated as permeable and periodic boundary conditions are imposed. The algorithm devised to simulate protein displacement involves randomly selecting a protein and attempting to move it by one lattice spacing in a random direction. If the move does not lead to overlap with neighbors, it is accepted. Otherwise it is rejected. Each attempted move is termed a “Monte Carlo step,” and typical simulations involve from  $10^5$  to  $10^7$  steps per particle.

During the simulation, the mean-square displacement of proteins from their starting positions is computed as a function of the number of steps attempted. Afterwards, a time interval is assigned

to each step, and a diffusion coefficient is extracted by assuming that the data obey Eq. (1)<sup>13,14,16-19</sup> or, alternatively, the relationship<sup>15</sup>

$$\langle r^2(t) \rangle = 4D^s t + A + B \ln(t). \quad (3)$$

The additional terms in Eq. (3) are attributed to the “long-time tail” of the two-dimensional velocity autocorrelation function.<sup>8</sup> Their effect is minimal at low concentrations, but they can reduce the diffusion coefficient by as much as 25% at high concentrations.<sup>15</sup>

The concentration dependence of  $D^s/D_0$  is determined by repeating the simulations for different protein concentrations. Two observations facilitate the presentation of data and serve to distance the results from the somewhat unphysical constraint of the lattice. First, although  $D_0$  depends on protein size, the ratio  $D^s/D_0$  is found to be nearly independent of size and essentially to be a function only of the area fraction,  $f_A$ , of membrane occupied by protein. Second, the ratio  $D^s/D_0$  is relatively insensitive to the structure of the lattice or the shape of the proteins.

**4.1.2 Results.** The mean-square displacement of proteins as a function of time and protein concentration is shown for the triangular lattice in Fig. 2. Note that if the expression  $\langle r^2 \rangle = 4D^s t$  (where  $D^s$  is independent of  $c$  and  $t$ ) were to hold,  $\langle r^2 \rangle$  would vary linearly with  $t$ . This is clearly not the case except at infinite protein dilution. Nevertheless, a relationship of the form given in Eq. (1) will still hold if we assume that the diffusion coefficient depends on time and concentration. Specifically, from Eq. (1) we can write  $D^s(c,t) = \langle r^2 \rangle / 4t$ . The data in Fig. 2 then show that the ratio  $D^s(c,t)/D_0$  assumes a value of unity at  $t = 0$  and then decays with time to a steady-state value,  $D_\infty^s(c)/D_0$ , which is determined by the protein concentration (area fraction) and which is independent of time. This same logic is used to extract a diffusion coefficient from Eq. (3).

The long-time values of the diffusion coefficient are plotted in Fig. 3 as a function of  $f_A$ . For convenience, they can be fit to a quartic polynomial<sup>15</sup>

$$D_\infty^s(f_A)/D_0 = 1 - 2.1187f_A + 1.8025f_A^2 - 1.6304f_A^3 + 0.9466f_A^4 \quad (4)$$

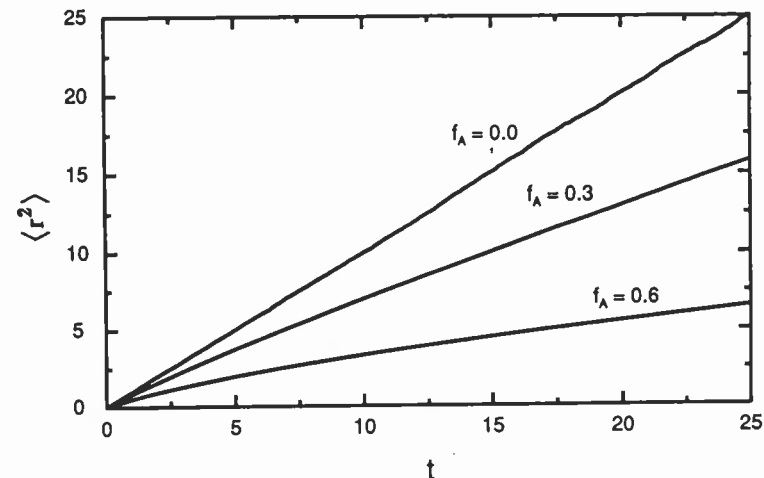


FIGURE 2 Mean-square displacement of proteins (in units of  $10^3$  lattice spacings) versus time (in units of  $10^3$  time steps) (not Monte Carlo steps/particle) on a triangular lattice; data are shown for three different area fractions,  $f_A = 0$ ,  $f_A = 0.3$ , and  $f_A = 0.6$ . The results were derived from a lattice-gas simulation of hexagonal proteins on a triangular lattice (Ref. 17). In the lattice-gas model,  $D_0 = \Lambda^2/(4\tau)$ , where  $\Lambda$  is the lattice spacing and  $\tau$  is the jump time. The following features of the data are worthy of note. When  $f_A = 0$ , there is a linear relationship between mean-square displacement and the time because at infinite dilution  $\langle r^2 \rangle = 4D_0 t$ , where  $D_0$  is independent of  $t$ . However, at finite area fractions, the linear relationship holds only for very *small* times and for *large* times: specifically,  $\langle r^2 \rangle = 4D_0 t$  and  $\langle r^2 \rangle = 4D_\infty^s(c)t$  in the short and long time limits, respectively. At intermediate times, the analogous relationship is  $\langle r^2 \rangle = 4D^s(c,t)t$ , where the extra temporal dependence appearing in the diffusion coefficient leads to the nonlinear relationship between mean-square displacement and time manifest in the figure. Finally, the curvature in the plots shows that the diffusion coefficient will *decay* monotonically with time.

to within 5% accuracy; no physical significance is attributed to the fit. The results indicate that long-time diffusion is significantly retarded by excluded-volume interactions: at area fractions of seventy-five percent, the long-time self-diffusion coefficient is about 1/20 of  $D_0$ .

**4.1.3. Critique.** The lattice-gas model has played a seminal role in theoretical analyses of concentration-dependent protein diffusion in membranes. As the first model applied to the problem, it defined the boundaries of the field. It is conceptually simple yet capable of yielding “exact” answers (within the confines of its starting assumptions). The simplicity of the model belies its con-

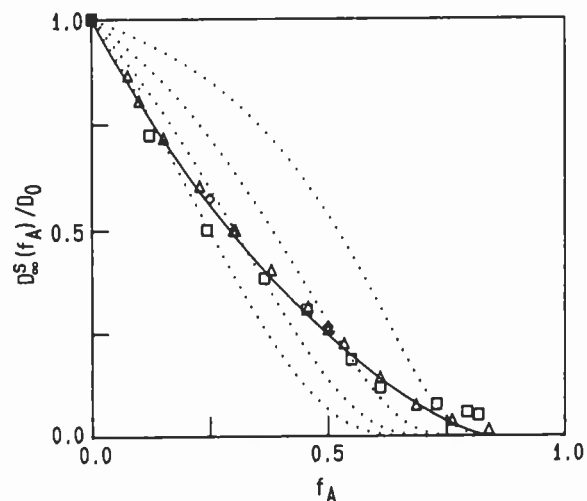


FIGURE 3 Long-time self-diffusion coefficients for proteins interacting through excluded-volume forces, at various area fractions of protein. The data points were determined using the lattice-gas model ( $\square$  Ref. 13;  $\triangle$  Ref. 15) and the Brownian model ( $\diamond$  Ref. 43). These values agree well with the best-fit lattice-gas expression given in Eq. (4) (—). The dashed curves represent the predictions of the free-volume model (Eq. (6)), when it is assumed that (right to left)  $x = 0.1, 0.2, 0.3,$  and  $0.4$ .

siderable power: with minor modifications, it has been generalized to treat lipid diffusion<sup>15,16,18,19,24</sup> and to describe systems containing immobile obstacles (see Section A.1), multiple protein species (see Section A.2), and cytoskeletal domains.<sup>25</sup> However, this largely numerical approach does not yield the physical insight or completeness of description that can be obtained from more detailed analytical analysis. For example, because it does not include any explicit reference to the membrane's lipid component, the lattice-gas model does not describe the influence of lipid dynamics on protein diffusion (see Section 5).

## 4.2. Free Volume Models

**4.2.1. Description of theory.** In lieu of appealing to numerical simulation, the free-volume model attempts to identify a rate-limiting step for diffusion and then to model the simplified rate-limiting process analytically. A final expression is obtained in closed

form. This approach builds upon the successful use of free-volume models to describe solvent diffusion in three-dimensional fluids<sup>26–28</sup> and lipid diffusion in membranes.<sup>1–3,29</sup> It is also closely related to free-volume models of protein diffusion in three-dimensional fluids.<sup>30,31</sup>

In the free-volume model, protein motion is assumed to take place in several steps. Incessant collisional interactions within the membrane give rise to fluctuations in protein concentration, including areas transiently devoid of protein, or “free volumes” (see Fig. 1c). (These fluctuations are also closely related to *mutual* diffusion.)<sup>32–34</sup> When such free volume is available, an adjacent protein can diffuse into it. This motion is assumed to take place without hindrance and at a rate dictated by  $D_0$ . The free volume is assumed to disappear as the fluctuation dissipates.

The rate of protein diffusion is determined by the probability of finding a free volume. Indeed, in this model the long-time self-diffusion coefficient is expressed as

$$D_{\infty}^s/D_0 = \exp(-\Delta G/RT) \quad (5)$$

where  $R$  is the gas constant and  $\Delta G$  is the work required to create a target area free of other proteins. The precise value of  $\Delta G$  depends upon the nature of the intermolecular interactions in the system and the geometry of the holes that allow diffusion. In free-volume models of solvent diffusion, it is typically assumed that an acceptable hole must be at least as large as a solvent molecule. In models of solute diffusion, this restriction is sometimes invoked<sup>30</sup> but can also be relaxed to allow motion into smaller spaces.<sup>31,35</sup> In all cases, the effects of interactions and geometry are not modeled exactly but are instead left as a free parameter that can be determined upon comparison with experiment. In free-volume models of lipid diffusion, there has been some attempt to relate this free parameter to specific properties of the membrane<sup>3</sup> or to recast it by renormalization.<sup>36</sup> The latter process may even improve agreement with experiment. Unfortunately, expressions modified in either manner have effectively only replaced one free parameter with another.

**4.2.2. Results.** In the free-volume model of membrane protein

diffusion, proteins were assumed to experience excluded-volume interactions and to be capable of movement into spaces smaller than individual proteins.<sup>35</sup> An analytical form for  $\Delta G$  was obtained from scaled-particle theory<sup>37</sup> and the long-time self-diffusion coefficient then written in the form

$$D_s^z(f_A)/D_0 = \exp[-x(4 + x)Q - x(2 + x)Q^2] \quad (6)$$

where  $Q \equiv f_A/(1 - f_A)$  and  $x (\leq 1)$  is essentially the free parameter mentioned above. The predictions of Eq. (6) are plotted in Fig. 3 for different choices of the free parameter. It is assumed that  $x$  can be adjusted by a least-squares fit when the free-volume model is applied to experimental data. The model predicts that as the protein concentration is increased, the probability of finding appropriate free volumes decreases, and, as a result, the self-diffusion coefficient is reduced. The results agree qualitatively but not quantitatively with the lattice-gas model.

**4.2.3. Critique.** The greatest strengths of the free-volume model are its attempt to identify a molecular mechanism for diffusion and its ability to yield analytical solutions. Another strength of the model is that it can be used to describe lipid diffusion and tracer protein diffusion among large and small proteins (see Section A.2). The greatest weakness of the model is that its validity is contingent upon the correctness of the assumed mechanism: that self-diffusion is rate limited by the formation of free volume. This postulate was first formulated for application to solvents, where the probability of hole formation is small; in the present context its validity is somewhat suspect, especially when the protein concentration is low and large free volumes can be expected. In addition, the predictions of the free-volume model are “soft” because they contain a free parameter. Finally, the free-volume model does not describe the temporal dependence of  $D^s$  nor the effects of lipid dynamics on protein diffusion (see Section 5).

### 4.3. Brownian Models

**4.3.1. Description of theory.** In the Brownian approach, the goal is to identify the molecular origins of the forces that act upon a diffusing particle and then to use this information to construct an

analytical model of diffusive motion. To date, the various interactions among solute and solvent have been assumed to translate into three types of forces on solute molecules: (i) Brownian interactions, which arise from collisions between solute and solvent, (ii) direct interactions between solute molecules, such as the excluded-volume interactions described above, and (iii) hydrodynamic interactions, which arise because the Brownian forces on neighboring solute particles are partially correlated and induce a flow in the solvent that affects other solute molecules.<sup>38,39</sup> These three interactions occur on different time scales and with different characteristic strengths;<sup>38,39</sup> however, they can have comparable effects on  $D^s$  and thus an adequate description of self-diffusion requires proper consideration of all three. Brownian models of membrane protein diffusion build upon a formidable theoretical apparatus that has evolved primarily to describe dynamic light scattering experiments in three-dimensional solutions.<sup>38-42</sup>

A direct implementation of the Brownian picture involves writing down a “Newtonian-style” equation of motion known as the Langevin equation,

$$m dv_i/dt = -f^s v_i + F_B(t) - \sum_{j \neq i} \nabla_i u_{ij}(r_{ij}) \quad (7)$$

where  $m$  and  $v_i$  are the mass and velocity of particle  $i$ , respectively,  $f^s$  is the self-friction coefficient,  $F_B(t)$  is the random Brownian force, and  $u_{ij}(r_{ij})$  is the interaction potential between Brownian particles  $i$  and  $j$  separated by a distance  $r_{ij}$ . The first two terms represent the Brownian interactions and the third direct interactions. Because the Brownian force is so complicated, it is defined only in a statistical sense, e.g.,  $\langle F_B \rangle = 0$ , where  $\langle \rangle$  denotes an ensemble average. In turn, only averaged properties of the trajectory of the solute particle can be calculated from the Langevin equation, e.g., the mean-square displacement  $\langle r^2 \rangle$  as a function of time. The diffusion coefficient is then determined from Eq. (1).

The expectation values, such as  $\langle r^2 \rangle$ , that one computes from the Langevin equation can also be calculated in a more familiar and equivalent fashion using appropriate probability distributions. The temporal and spatial dependence of these distribution func-

tions are dictated by “generalized diffusion equations,” an example of which is the Smoluchowski equation

$$\partial P_N / \partial t = D_0 \sum_i \nabla_i \cdot \{ \nabla_i P_N + 1/(k_B T) \sum_{j \neq i} (\nabla_i u_{ij}) P_N \}. \quad (8)$$

Here  $P_N$  is an  $N$  particle distribution function describing the probability of finding particles  $1 - N$  at positions  $\{r_1 - r_N\}$ . Although this equation is formidable in appearance, it reduces to a “typical” diffusion equation in the absence of interactions, i.e., when  $u_{ij} = 0$ .

**4.3.2. Results.** The Brownian approach has been used to describe membrane protein diffusion, initially in the absence of hydrodynamic interactions.<sup>32,43</sup> Using a combination of the approaches described in Section 4.3.1, an expression for the long-time self-diffusion coefficient was derived:

$$D_{\infty}^s(\rho)/D_0 = 1 + (\rho\pi/2k_B T) \int [du(r)/dr]g(r,\rho)p(r,\rho)rdr \quad (9)$$

where  $\rho$  is the number density of proteins,  $g(r,\rho)$  is the two-particle radial distribution function describing protein order in the system, and  $p(r,\rho)$  is a radial perturbation function that is obtained as the solution of an integrodifferential equation (not shown). An expression for the short-time diffusion coefficient (not shown) was also obtained from Brownian theory. It too is analytical. Unfortunately, probability distributions such as  $g(r,\rho)$  that enter into these equations are usually not known in analytical form; instead, they must be determined numerically by continuum Monte Carlo simulations. Equation (9) must then be evaluated numerically.

The Brownian model has been used to study the effects of excluded-volume interactions on long- and short-time self-diffusion (see Fig. 3). These results are essentially in exact agreement with the predictions of the lattice-gas model. The Brownian model has also been used to determine the effects that long-range inverse-power-law repulsions and attractions have on diffusion (see Fig. 4). Here again the diffusion coefficient was found to decay monotonically with time and protein concentration in both the presence and absence of the long-range attraction. In fact, for all potentials

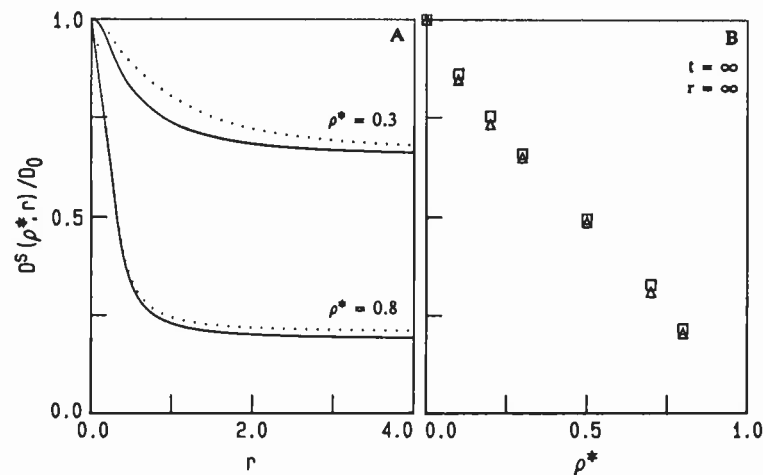


FIGURE 4 Short-time (A) and long-time (B) self-diffusion coefficients for proteins interacting through long-range attractive and repulsive protein-protein interactions, at various concentrations of protein. These results were obtained by applying the Brownian model to purely repulsive ( $\cdots$  and  $\square$ ) and attractive-plus-repulsive ( $—$  and  $\Delta$ ) interactions (Ref. 43). Functional forms for these potentials are defined in Ref. 43; concentrations are expressed in terms of the reduced density of protein,  $\rho^*$ , rather than the area fraction,  $f_A$ . Panel A shows the distance dependence of the self-diffusion coefficient for  $\rho^* = 0.3$  and  $\rho^* = 0.8$ . The temporal dependence of  $D^s(c,t)$  was converted into a spatial dependence by computing displacement,  $r = \langle r^2 \rangle^{1/2}$ , from the relationship  $\langle r^2 \rangle = 4D^s(c,t)t$ . The average interparticle separation at both densities corresponds to  $r \approx 1$ . Panel B shows the density dependence of the long-time self-diffusion coefficient. Note that, despite the differences in the potentials, the diffusion coefficients for the two systems are very similar. Nevertheless, small systematic discrepancies are manifest. For example, for a given repulsive interaction, the long-time value of the self-diffusion coefficient is always smaller when the interaction also has an attractive component. This result may reflect the fact that attractions tend to hold particles together and retard their movement or, alternatively, the fact that the precise arrangement of particles differs for the two potentials (Ref. 43). Also note that, at low density, the diffusion coefficient for the attractive potential falls off more rapidly with displacement than does the diffusion coefficient for the purely repulsive potential; this is related to the fact that neighboring particles are in closer proximity in the attractive fluid (Ref. 43) and so act more quickly to cage a diffusor. Finally, for both of these long-range interactions and the excluded-volume interactions in Fig. 3, each additional incremental increase in protein density produces a smaller incremental decrease in the self-diffusion coefficient. This observation supports the concept of “caging”: at low densities each additional protein contributes to the cage, but at higher densities each additional protein is partially blocked by other proteins and so is less effective at caging motion.

analyzed to date, the diffusion coefficient manifests essentially the same temporal and concentration dependence; minor differences are noted in the figure. The interaction dependence of the diffusion coefficient can be understood as follows. Attractive interactions inhibit diffusion by loosely tethering molecules to their neighbors. In contrast, repulsive interactions inhibit diffusion by increasing the effective size (and thus the effective area fraction) of the particles. Thus, appending either long-range attractions or repulsions onto excluded-volume interactions will probably tend to retard diffusion even more than the excluded-volume interaction alone does.

**4.3.3. Critique.** The Brownian model is the most powerful theoretical approach used to study concentration-dependent protein diffusion in membranes. It has proven successful at describing solute diffusion in three-dimensional fluids<sup>38</sup> and protein diffusion in dilute membranes (through the Saffman–Delbrück equation).<sup>2</sup> It can be generalized to describe the effects of the solvent on solute diffusion (see Section 5) and to describe diffusion in systems containing multiple solute species (see Section A.2). Finally, the temporal dependence of  $D^s$  is best described by the Brownian theory because the free-volume model is not applicable to this problem and the lattice-gas model is limited in spatial resolution by the lattice. The primary disadvantage of the Brownian approach is that analytical expressions such as Eq. (9) require information best obtained from numerical (Monte Carlo) simulation. Brownian models also are not applicable to lipid diffusion, since postulating the existence of a Brownian force, which arises when a particle is rapidly bombarded by solvent, is reasonable only if the diffusing particle is much larger than the solvent.

#### 4.4. Summary and Interpretation

The predictions of these three models can be synthesized into a fairly consistent and intuitively reasonable picture of the effects that direct interprotein interactions have on protein diffusion in simple concentrated membranes. Focus attention on one protein within the membrane. Instantaneously, the motion of this particle is dictated only by its interactions with the solvent (because solvent–solute interactions are stronger than solute–solute interac-

tions),<sup>38</sup> and the diffusion coefficient is given by its value in dilute solution,  $D_0$ . At longer times,  $t$  (or, equivalently, after the particle has undergone a larger displacement,  $\langle r^2 \rangle = 4D^s t$ ), the diffusor encounters (and interacts with) other proteins, and the description given by  $D_0$  is no longer adequate. Instead, a diffusion coefficient satisfying Eq. (1) must vary with time (or displacement); specifically, the diffusion coefficient decays monotonically with time (or distance) from  $D_0$  to a time-independent, long-time value,  $D_\infty^s(c)$ . This decay occurs after just a few interactions with other proteins.

The long-time value of the self-diffusion coefficient decreases markedly with increasing protein concentration. For the hard-disk fluid, the decrease is a fewfold at fifty percent area fraction and up to twentyfold at seventy-five percent area fraction. In fact, for all forms of the interprotein force studied to date,  $D_\infty^s(c)/D_0$  manifests essentially the same concentration dependence and depends primarily upon the “effective” area fraction occupied by the protein. Taken together, these observations suggest that the following molecular mechanism is the primary determinant of the concentration dependence of  $D_\infty^s(c)$ : neighboring proteins transiently “cage” a diffusor and thereby inhibit its motion. Since the degree of caging increases with increasing protein concentration, the self-diffusion coefficient is largest when the system is dilute and interactions are negligible, and then decreases as concentration increases.

## 5. UNRESOLVED THEORETICAL ISSUES

Although the three rather disparate theoretical approaches described above yield a reasonably consistent picture of the effects that direct *protein–protein* interactions have on the self-diffusion of membrane proteins, at least three additional *lipid–protein* interactions must be incorporated into the theoretical descriptions before they are truly complete. These are protein-induced changes in the protein–protein force and membrane viscosity, and hydrodynamic interactions.

### 5.1. Protein-Induced Perturbations in the Protein–Protein Force and Viscosity

Membrane proteins can perturb the conformation and dynamics of membrane lipids.<sup>44,45</sup> Such changes around an isolated protein

are implicitly incorporated into Eq. (2) because the membrane viscosity appearing therein will reflect the perturbation. However, as the concentration of protein is increased, the annuli of perturbed lipids surrounding different proteins could overlap. This overlap is predicted to create concentration-dependent lipid-mediated protein–protein interactions,<sup>46</sup> and it could impart a concentration dependence to the membrane viscosity.<sup>15,43</sup> These two effects potentially need to be incorporated into descriptions of interaction-dependent membrane protein diffusion.

Lipid-mediated interactions can be incorporated into the theories presented in Section 4 by allowing the interprotein force to vary with protein density. If this were done we would expect, for example, that a repulsive lipid-mediated force with a range that increases with density would cause  $D^s$  to fall off more rapidly with concentration than would a comparable density-independent force.

Changes in viscosity that are induced by high protein concentration are difficult to treat theoretically because the molecular origin of membrane viscosity is poorly understood. Nevertheless, such changes can be treated phenomenologically by inserting a concentration-dependent viscosity into the expression for  $D_0$ , Eq. (2). If this procedure is implemented, the decrease in  $D^s$  that results from direct interparticle interactions will be augmented by an increase in viscosity and countered by a decrease in viscosity.<sup>43†</sup>

## 5.2. Hydrodynamic Interactions

Protein motion is necessarily accompanied by lipid movement, e.g., lipids are pushed ahead and pulled behind a moving protein. This solute-correlated solvent motion sets up forces in the fluid that can propagate and affect the motion of other solute particles. Such “hydrodynamic interactions” have been well studied in three-dimensional systems,<sup>38,39</sup> but have been neglected in the theories presented above. Although they cannot easily be incorporated into the lattice-gas and free-volume models, hydrodynamic interactions can be incorporated into the Brownian model if a form for the hydrodynamic tensor is known.

Unfortunately, a tensor describing the hydrodynamic interaction between particles constrained to move in two dimensions has not been derived, to date; this derivation would parallel, in many

respects, that of the Saffman–Delbrück equation. Nevertheless, preliminary analyses (Scalettar and Abney, unpublished results) using tensors describing three-dimensional systems suggest that hydrodynamic interactions have comparable effects on diffusion in two and three dimensions. Hydrodynamic effects are minimal in dilute solutions in which the interaction is of long-range, but become increasingly significant as concentration increases.

## 6. COMPARISON OF THEORY WITH EXPERIMENT

The goal of theory is to provide a simple and unified explanation for experimental observations. Thus, this paper would be patently incomplete without a comparison between theory and experiment. In this section, we will discuss experiments that address the concentration dependence of the two-dimensional self-diffusion coefficient. Unfortunately, as we shall see, none of the experimental systems described herein possess all of the characteristics of the theoretical model system. Nevertheless, by discussing experiments on a number of systems, the agreement between theory and experiment can be fairly well assessed.

### 6.1. Self-Diffusion and Experimental Methods

The diffusion of membrane proteins has been studied experimentally with a variety of techniques. These methods are sensitive to different types of diffusion and to diffusion over different time scales.<sup>32</sup> Two of these methods, nanometer-level video microscopy and fluorescence recovery after photobleaching (FRAP), are particularly germane to our discussion because they yield a self-diffusion coefficient.

Nanometer-level video microscopy permits the displacement of individual molecules to be followed as a function of time<sup>47</sup> and thus is essentially an experimental analogue of a lattice gas simulation. The trajectory of a particle is visualized by labeling it with a fluorescent probe or colloidal gold. If the observed motion is completely random, a self-diffusion coefficient can be extracted from Eq. (1) by dividing the measured mean-square displacement by four times the time. In addition, nondiffusive motion of a par-

ticle can be detected. In principle, this technique can be used to monitor both the concentration and time dependence of the self-diffusion coefficient.

A more commonly used technique is fluorescence recovery after photobleaching (FRAP).<sup>48–52</sup> In a FRAP experiment, the diffusion of many molecules is monitored simultaneously by measuring the rate at which fluorescence returns to a bleached region of a sample. Since the spatial resolution of FRAP is limited to about one micron, the technique monitors long-range diffusion that is averaged over many interactions and can thus yield  $D_{\Sigma}^{\pm}$  as a function of concentration.

### 6.2. Experimental Measurements: Video Microscopy

Video microscopy has recently been used to monitor the self-diffusion of nonspecifically labeled membrane glycoproteins, Thy-1, and the LDL receptor on living cells.<sup>53–57</sup> The analyses have revealed evidence for various modes of motion in cells, including (i) random, Brownian motion, (ii) percolation, and (iii) directed motion. Video microscopy has also shown that, in some cellular systems, the self-diffusion coefficient decays with time. However, this decay in  $D^{\pm}$  occurs on a time scale that reflects the “corralling” of particles into micron-sized domains rather than the “caging” of particles on interparticle distance scales discussed previously (see Section 4.4). Detection of this latter, very short-range, diffusive motion will have to await improvements in the temporal or spatial resolution of video microscopy. Finally, we note that video microscopy has not, to date, been used to study (concentration-dependent) diffusion in relatively simple systems. However, it is likely that video tracking in model systems, such as those consisting of individual gold-labeled antibodies tethered to lipid haptens in supported planar lipid bilayers,<sup>58</sup> will soon provide interesting new insights into the physical mechanisms of diffusion (see also Section 6.3.2).

### 6.3. Experimental Measurements: FRAP

To date, only FRAP has been used to study the concentration dependence of the two-dimensional self-diffusion coefficient. In this section we discuss FRAP experiments on surface-adsorbed

proteins, lipid-bound antibodies and synthetic peptides, and integral membrane proteins.

*6.3.1. Surface-adsorbed proteins.* At this point it is important to emphasize that the models discussed herein are applicable not just to membranes but to any appropriate two-dimensional system. Indeed, the only experiments that have been specifically designed to test these theories were conducted on bovine serum albumin adsorbed from aqueous solution onto poly(methylmethacrylate)-coated surfaces.<sup>59</sup> The self-diffusion coefficient of the albumin was found to be a monotonically decreasing function of protein concentration. At an area fraction of about 70%, the self-diffusion coefficient was about 1/10 of  $D_0$ . Both of these observations agree qualitatively with theoretical predictions. Unfortunately, this system contains a substantial ( $\approx 60\%$ ) immobile fraction. The results are thus more correctly described by theories that take the immobile population into account (see Section A.1).

*6.3.2. Lipid-bound antibodies and synthetic peptides.* The concentration-dependent self-diffusion of antibodies bound to lipid haptens at the surface of planar lipid monolayers and bilayers has also been investigated.<sup>60–62</sup> Binding constrains the antibodies to move in two dimensions, and they interact with one another through the aqueous medium. In each study, the self-diffusion coefficient was found to decrease with increasing antibody concentration. In some cases, the decrease in  $D_{\Sigma}^{\pm}$  is partially a consequence of aggregation.<sup>62</sup> In others, a two-to-threefold decay in  $D_{\Sigma}^{\pm}$  at concentrations up to saturation may represent the effects of interactions alone.<sup>61</sup> For the antibody system, the data are again in qualitative accord with theory; unfortunately, they cannot be quantitatively compared with theory because the area fractions of antibody were not quantified. It is worth noting, however, that concentration has a less pronounced effect on antibody diffusion than on adsorbed albumin diffusion, perhaps because the immobile fractions are lower in the antibody system.

A similar concentration dependence was obtained for the diffusion coefficients of synthetic peptides covalently linked to a membrane lipid and reconstituted into supported phospholipid monolayers.<sup>63</sup> The diffusion coefficients of three different peptide-lipids

were reduced up to fourfold at 11 mole-percent "protein". The mobile fractions in this system were less than 70%.

6.3.3. *Integral membrane proteins.* Diffusion coefficients for gramicidin and bacteriorhodopsin were measured for proteins reconstituted into simple, phosphatidylcholine vesicles and multibilayers.<sup>1,64,65</sup> The diffusion coefficients of both proteins decreased substantially as concentration was increased. For these systems, we can make a fairly detailed comparison with theory because the mobile fractions of the molecules were high and the relevant area fractions can be calculated. Unfortunately, precise comparison between theory and experiment hinges on a knowledge of the protein-protein force, which is unavailable for gramicidin and which has only been characterized indirectly for bacteriorhodopsin.<sup>66</sup> In the absence of detailed information about forces, a reasonable comparison between theory and experiment can still be made using the prototypical excluded-volume interaction. Such an analysis (see Fig. 5) suggests that excluded-volume interactions can account for part, but not all, of the concentration dependence of the self-diffusion coefficient in the gramicidin and bacteriorhodopsin systems.<sup>11</sup> Part of the disparity between theory and experiment may reflect protein aggregation at high protein concentration, particularly in the case of bacteriorhodopsin.<sup>65</sup> Alternatively, protein-induced perturbation of lipid or the existence of (a static or dynamic layer of) boundary lipid that increases the effective size of protein could lead to disagreement between theory and experiment.<sup>15,18,19</sup>

The concentration dependence of the self-diffusion coefficient of Complex III in mitochondrial inner membranes has also been measured.<sup>67</sup> It was found that as the protein concentration was reduced by fusion of liposomes, the diffusion coefficient of Complex III increased. A sevenfold protein dilution gave rise to a twentyfold increase in the diffusion coefficient. The mobile fraction in this system is high (> 85%); however, mitochondrial membranes contain many species of protein and so are probably best described by theories that take multiple solute species into account (see Section A.2).

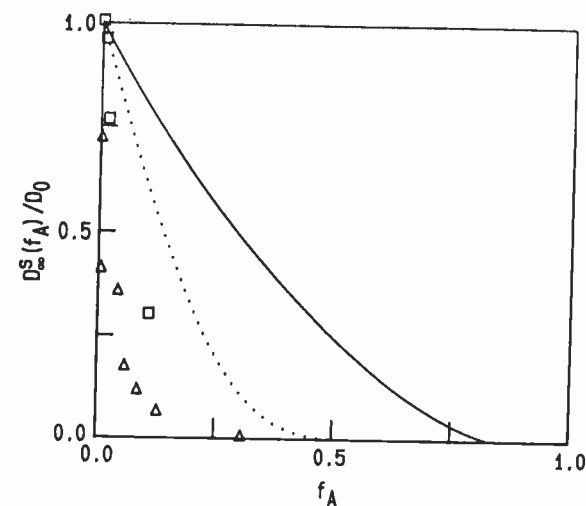


FIGURE 5 Comparison of long-time self-diffusion coefficients for gramicidin ( $\square$  Ref. 64) and bacteriorhodopsin ( $\Delta$  Refs. 1 and 65) with theoretical predictions for the excluded-volume interaction. Area fractions were determined as described previously (Refs. 15 and 17); values for  $D_0$  were determined by extrapolating the experimental values back to  $f_A = 0$  using a simple polynomial fit (Ref. 83) (Fitting can be avoided by using a log/log plot (Ref. 15); however, such a plot obscures somewhat the comparison between theory and experiment.) The theoretical curves (defined as in Fig. 3) are taken from Eq. (4), which fit the lattice-gas and Brownian models, and Eq. (6), which describes the free-volume model. Two significant areas of agreement between theory and experiment are worthy of note. First, the self-diffusion coefficient decreases with increasing protein concentration. Second, the rate of the decay in  $D_{\infty}^S$  decreases with increasing protein concentration (see Fig. 4). Note that the free-volume results are in closer agreement with experiment than the lattice-gas and Brownian results. However, the significance of this observation is not clear because the free-volume model contains a free parameter (here taken to be 1 to maximize agreement with experiment) that is not present in the other two theories.

#### 6.4. Experimental Measurements: Electron Microscopy

The effects that interactions have on the diffusion of proteins in murine liver gap junctions were "measured" in a somewhat different manner.<sup>43</sup> In this study, the protein-protein force and distribution functions describing protein order in the gap junction were determined from particle positions revealed in freeze-fracture

electron micrographs.<sup>68,69</sup> This information was then used to evaluate Eq. (9) for  $D_{\pm}^s$ . It was found that protein-protein forces in the gap junction reduce the diffusion coefficient by about twofold at approximately 30% area fraction of protein.

### 6.5. Summary and Interpretation

The results described in Sections 6.3 and 6.4 demonstrate quite unequivocally that the experimental long-time two-dimensional self-diffusion coefficient is a decreasing function of protein concentration. Moreover, the theoretical analyses described in this article also demonstrate quite clearly that one can qualitatively (but perhaps not quantitatively) explain the experimentally observed concentration dependence of  $D_{\pm}^s$  by assuming that the solute particles interact through simple direct forces. Quantitative disparities between theory and experiment could reflect shortcomings in the theories, such as the neglect of hydrodynamic interactions, viscosity changes, or other effects not yet identified. They may also reflect differences between real experimental systems and the ideal systems described by theory, or experimental errors such as inaccurate calculations of protein concentrations. In fact, it is worth noting that an error of a factor of two or three in protein concentration would completely account for the disparity apparent in Fig. 5.

It is clear that there is still room for additional experimental study of interaction-dependent membrane protein diffusion. Future experimental work could be directed at more rigorous measurement of the concentration dependence of the long-time self-diffusion coefficient. In an ideally designed experiment, the inter-protein force would be measured, area fractions would be accurately calculated, and the system under study would manifest no aggregation, immobile fraction, or phase separation. If previous experimental results are any indication, it may be difficult to construct an ideal system. Alternatively, an attempt could be made to measure the predicted time dependence of the self-diffusion coefficient, using video microscopy or perhaps collisional techniques. Such “new data” would probably provide stronger confirmation of the theories. Whatever measurements are made, additional data will strengthen the qualitative conclusions already reached

and will better define the “typical” experimental system that theorists should aim to describe.

## 7. CONCLUSIONS

Both the theoretical and experimental work described herein demonstrate that the self-diffusion of membrane proteins is retarded at high protein concentrations. In simple systems containing lipid and one species of mobile protein, the decrease in diffusive rate is probably a few to tenfold at physiological protein concentrations. Current models of membrane protein diffusion in concentrated systems assume that the proteins interact only through direct, e.g., excluded-volume, forces and, given this starting assumption, are capable of qualitatively reproducing experimental data. However, quantitative comparison of theory and experiment suggests that current theoretical descriptions are somewhat incomplete and that indirect, solvent-mediated interactions should be incorporated into them to improve agreement with experiment.

## APPENDIX

The simple models discussed here will have to be generalized before they can be applied to real biological membranes. How might the predictions of theory be altered once the complexity of the biomembrane has been tackled? In biological membranes, a protein usually interacts not just with one type of protein but with multiple species of proteins, immobile proteins, and extramembraneous structures. To date, no theory has attempted to describe all such potential interactions simultaneously; however, we would like to mention briefly some predicted features of diffusion in either the presence of immobile proteins or in multicomponent systems.

### A.1. Immobile Obstacles and Percolation

Diffusion in membranes containing immobile proteins or large impermeant domains has been modeled with a variety of approaches.<sup>15-17,24,70,71</sup> Undoubtedly the most powerful of these ap-

proaches is percolation theory.<sup>72,73</sup> In the percolation model, the membrane surface is divided into two types of regions: obstacles and vacancies. Mobile tracer molecules, which are present at very low concentration, are confined to the vacancies, and their motion in the presence of *immobile* obstacles is monitored. Percolation theory predicts that the diffusion coefficient of the mobile species is always  $\leq D_0$ , just as the theories of diffusion in the presence of mobile (protein) obstacles do.

However, diffusion among immobile obstacles differs in at least two important respects from diffusion among mobile obstacles. First, at low concentrations of immobile obstacles, all vacancies are connected, and in the long-time limit the mean-square displacement goes to infinity. However, at high concentrations of immobile obstacles, vacancies become isolated (i.e., entirely surrounded by obstacles), and long-range diffusion is blocked. The latter behavior is first manifest at the “percolation threshold,” i.e., when the last long-range path for diffusion is blocked. Although the percolation threshold depends on the geometry of the lattice (or continuum) and on the geometry of the obstacles, it usually occurs at a few tens of percent area fraction of immobile obstacles. It is sometimes forgotten that the percolation threshold exists only in the presence of immobile obstacles. When all the obstacles are mobile, long-range diffusion is not blocked.<sup>15</sup>

Second, when immobile obstacles are present the mean-square displacement is no longer a linear function of  $t$ , but instead varies as  $t^{2/d_w}$ , where the diffusion exponent  $d_w > 2$ .<sup>22,72,73</sup> In this case, the mean-square displacement increases less rapidly with time because particles are delayed amid the complicated static pathways and dead ends formed by the obstacles. This result should be contrasted with earlier beliefs that impermeant domains would “canalize” long-range diffusion and thus enhance it.<sup>74</sup>

Very recently, diffusion in systems containing both mobile and immobile proteins has been analyzed using Monte Carlo methods.<sup>17</sup> Such systems are intermediate between those described using percolation theory (all obstacles immobile) and those described using the theories in Section 4 of this article (all obstacles mobile). In this study, diffusion coefficients were obtained as a function of the area fraction of mobile protein, for different total area fractions of protein. (Total area fraction is just the sum of the mobile and

immobile fractions.) The diffusion coefficient again is found to decrease as the total area fraction of obstacles increases. Moreover, for a fixed total area fraction of obstacles, the diffusion coefficient is largest when all obstacles are mobile and smallest when they are all immobile. Between these two extrema, the diffusion coefficient decays monotonically as the area fraction of immobile particles increases.

## A.2. Multicomponent Membranes

Protein diffusion in membranes containing two unlike (e.g., large and small) species of mobile protein has been examined using the lattice-gas<sup>19</sup> and free-volume<sup>35</sup> models. Brownian theory has only been used to study diffusion in binary solutions that are *three* dimensional.<sup>75</sup> The same qualitative results were obtained from all three models. The self-diffusion coefficient of both species is always less than or equal to the appropriate  $D_0$ . Moreover, for a fixed total area/volume fraction of solute, an increase in the fraction of large particles increases the self-diffusion coefficient of small particles; conversely, an increase in the fraction of small particles decreases the self-diffusion coefficient of large particles.

At first glance, it might appear that an increase in the area fraction of larger (i.e., slower) particles should inhibit, rather than accelerate, self-diffusion. However, two small particles whose area is equivalent to one large particle can, in fact, block a larger area than the equivalent large particle. Therefore, since path blockage seems to be the primary cause of the inhibition of self-diffusion (see Section 4.4), the results obtained from the multicomponent analyses seem physically reasonable.

## Acknowledgments

We are pleased to acknowledge helpful conversations on diffusion with Daniel Axelrod, Ken Jacobson, John Owicki, Michael Saxton, J. Michael Schurr, Nancy Thompson, Winchil Vaz, and Watt Webb. In addition, Ken Jacobson and Michael Saxton provided detailed and useful comments on the manuscript. We thank Michael Saxton for providing Fig. 2 and Arthur Palmer, Mary Lee Pisarchick, and Nancy Thompson for their assistance in preparing Figs. 3, 4, and 5.

BETHE A. SCALETTAR and JAMES R. ABNEY  
*Laboratories for Cell Biology,  
Department of Cell Biology & Anatomy,  
University of North Carolina,  
Chapel Hill, North Carolina 27599*

Footnotes

\* Self-diffusion is to be contrasted with *mutual* diffusion, which refers to the dissipation of fluctuations or gradients in protein concentration.<sup>32-34</sup> Another type of diffusive motion, *tracer* diffusion, should also be mentioned here. Suppose that a solution contains a relatively numerous unlabeled solute species and a relatively dilute labeled solute species; the labeled species is assumed to be nonuniformly distributed but is otherwise indistinguishable from its unlabeled counterpart. Tracer diffusion refers to the diffusion of the labeled species in such a sample. It can be demonstrated that, under many conditions of interest, the tracer- and self-diffusion coefficients are equal.<sup>39</sup> Therefore, the terms self- and tracer diffusion are sometimes used interchangeably.

<sup>†</sup> The most noteworthy feature of Eq. (1) is the linear relationship between the mean-square displacement and the time. Such a linear relationship will hold whenever a molecule is executing random-walk-like motion, e.g., a drunkard's walk on a lattice,<sup>76</sup> or classic Brownian motion in solution.<sup>77</sup> However, if the motion is not random but instead obeys the laws of classical mechanics, the mean-square displacement will vary as  $t^2$ .<sup>77</sup> If a random walk is superimposed upon directed classical motion, then  $\langle r^2 \rangle$  will depend on both  $t$  and  $t^2$ . Finally, if the system contains immobile obstacles, the mean-square displacement will vary as  $t^{d_w}$ , where  $d_w \neq 1$  or 2 (see Section A.1).

<sup>‡</sup> Although self- and mutual-diffusion coefficients are in general different at finite protein concentration, at infinite dilution they are the same.<sup>32</sup> Thus, the discussion in this section is applicable to both forms of diffusion.

<sup>§</sup> The long-time tail in Eq. (3) can be rationalized physically, as follows. In the absence of interparticle interactions, particles can execute a truly random walk, and the statistical description of their motion is given in Eq. (1). However, if the diffusing particles are interacting with one another, their motion is partially determined by nonrandom (e.g., non-Brownian) forces, and their "random walk" is not, in fact, completely random. It is the nonrandom character of the motion of interacting particles that gives rise to the extra terms in Eq. (3).

<sup>¶</sup> In Section 5.1 it was noted that high protein concentration could perturb the *microscopic* shear viscosity of the membrane and thus alter the self-diffusion coefficient of membrane proteins. Here we note that high solute concentrations have been shown to alter the *macroscopic* shear viscosity of a fluid, i.e., the response of a fluid to an externally applied shear force.<sup>79</sup> Specifically, both experiment and theory indicate that the macroscopic shear viscosity depends on solute concentration, the solute-solute force, and the time,<sup>79</sup> much as the self-diffusion coefficient does. Unfortunately, since microscopic and macroscopic viscosities are not necessarily the same, the concentration dependence of the microscopic viscosity cannot be deduced from that of the macroscopic viscosity. Previous discussions of protein-induced perturbations in membrane viscosity have not noted this point.<sup>2,65,80</sup>

<sup>||</sup> It is interesting to note that the effect of protein concentration on *lipid* diffusion

is also underestimated by theory.<sup>15,81</sup> It is tempting to speculate that the systematic theoretical underestimates of the effect of protein concentration on both protein and lipid diffusion have common origins. Theories of lipid diffusion among protein obstacles have been briefly reviewed.<sup>81</sup>

References

1. W. L. C. Vaz, F. Goodsaid-Zalduondo and K. Jacobson, *FEBS Lett.* **174**, 199 (1984).
2. R. M. Clegg and W. L. C. Vaz, in *Progress in Protein-Lipid Interactions*, eds. A. Watts and J. J. H. M. de Pont (Elsevier, Holland, 1985), pp. 173-229.
3. K. Beck, in *Cytomechanics*, eds. J. Berciter-Hahn, O. R. Anderson and W.-E. Reif (Springer-Verlag, Heidelberg, Berlin, 1987), pp. 79-99.
4. M. P. Sheetz, *Sem. Hematol.* **20**, 175 (1983).
5. D. Kell, *Trends Biochem. Sci.* **9**, 86 (1984).
6. B. Gumbiner and D. Louvard, *Trends Biochem. Sci.* **10**, 435 (1985).
7. K. Jacobson, A. Ishihara and R. Inman, *Annu. Rev. Physiol.* **49**, 163 (1987).
8. S. J. Singer and G. L. Nicolson, *Science* **175**, 720 (1972).
9. P. G. Saffman and M. Delbrück, *Proc. Natl. Acad. Sci. USA* **72**, 3111 (1975).
10. P. G. Saffman, *J. Fluid Mech.* **73**, 593 (1976).
11. B. D. Hughes, B. A. Pailthorpe and L. R. White, *J. Fluid Mech.* **110**, 349 (1981).
12. F. W. Wiegel, *Lecture Notes in Physics*, Vol. 121 (Springer-Verlag, New York, 1980).
13. D. A. Pink, *Biochim. Biophys. Acta* **818**, 200 (1985).
14. D. A. Pink, D. J. Laidlaw and D. M. Chisholm, *Biochim. Biophys. Acta* **863**, 9 (1986).
15. M. J. Saxton, *Biophys. J.* **52**, 989 (1987).
16. M. J. Saxton, *Biophys. J.* **56**, 615 (1989).
17. M. J. Saxton, *Biophys. J.* **58**, 1303 (1990).
18. P. J. Donaldson, *Modulation of Lateral Diffusion on Lipid Bilayer Membranes* (Ph.D. Thesis, Cornell University, 1989).
19. P. J. Donaldson and W. W. Webb, *Biophys. J.* **53**, 121a (Abstract) (1988).
20. K. W. Kehr and K. Binder, in *Applications of the Monte Carlo Method in Statistical Physics*, ed. K. Binder (Springer-Verlag, Berlin, 1984), pp. 181-221.
21. J. W. Haus and K. W. Kehr, *Phys. Rep.* **150**, 263 (1987).
22. S. Havlin and D. Ben-Avraham, *Adv. Phys.* **36**, 695 (1987).
23. R. A. Tahir-Kheli and N. El-Meshad, *Phys. Rev. B* **32**, 6166 (1985).
24. J. Eisinger, J. Flores and W. P. Petersen, *Biophys. J.* **49**, 987 (1986).
25. M. J. Saxton, *Int. J. Biochem.* **22**, 801 (1990).
26. M. H. Cohen and D. Turnbull, *J. Chem. Phys.* **31**, 1164 (1959).
27. P. B. Macedo and T. A. Litovitz, *J. Chem. Phys.* **41**, 245 (1965).
28. G. S. Grest and M. H. Cohen, *Adv. Chem. Phys.* **48**, 455 (1981).
29. H. J. Galla, W. Hartmann, U. Theilen and E. Sackmann, *J. Membr. Biol.* **48**, 215 (1979).
30. T. J. O'Leary, *Biophys. J.* **52**, 137 (1987).
31. N. Muramatsu and A. P. Minton, *Proc. Natl. Acad. Sci. USA* **85**, 2984 (1988).

32. B. A. Scalettar, J. R. Abney and J. C. Owicki, Proc. Natl. Acad. Sci. USA **85**, 6726 (1988).
33. J. R. Abney, B. A. Scalettar and J. C. Owicki, Biophys. J. **56**, 315 (1989).
34. J. R. Abney, B. A. Scalettar and C. R. Hackenbrock, Biophys. J. **58**, 261 (1990).
35. P. Minton, Biophys. J. **55**, 805 (1989).
36. T. F. Nonnenmacher, Eur. Biophys. J. **16**, 375 (1989).
37. J. L. Lebowitz, E. Helfand and E. Praestgaard, J. Chem. Phys. **43**, 774 (1965).
38. P. N. Pusey and R. J. A. Tough, in *Dynamic Light Scattering Applications of Photon Correlation Spectroscopy*, ed. R. Pecora (Plenum, New York, 1985), pp. 85–179.
39. J. M. Rallison and E. J. Hinch, J. Fluid Mech. **167**, 131 (1986).
40. G. K. Batchelor, J. Fluid Mech. **74**, 1 (1976).
41. Faraday Division, Royal Society of Chemistry, *Concentrated Colloidal Dispersions*, Faraday Discuss. Chem. Soc. **76** (1983).
42. Faraday Division, Royal Society of Chemistry, *Brownian Motion*, Faraday Discuss. Chem. Soc. **83** (1987).
43. J. R. Abney, B. A. Scalettar and J. C. Owicki, Biophys. J. **55**, 817 (1989).
44. P. C. Jost and O. H. Griffith (Eds.), *Lipid-Protein Interactions*, Vol. 2 (Wiley, New York, 1982).
45. A. Watts and J. J. H. M. de Pont (Eds.), *Progress in Protein-Lipid Interactions*, Vol. 1 (Elsevier, Amsterdam, 1985).
46. J. R. Abney and J. C. Owicki, in *Progress in Protein-Lipid Interactions*, eds. A. Watts and J. J. H. M. de Pont (Elsevier, Holland, 1985), pp. 1–60.
47. H. Geerts, M. de Brabander, R. Nuydens and R. Nuyens, Comments Mol. Cell. Biophys. **5**, 279 (1988).
48. G. D. J. Phillis, Biopolymers **14**, 499 (1975).
49. R. Peters, Cell Biol. Int. Rep. **5**, 733 (1981).
50. W. L. C. Vaz, Z. I. Derzko and K. A. Jacobson, in *Membrane Reconstitution*, eds. G. Poste and G. L. Nicolson (Elsevier, Holland, 1982), pp. 83–136.
51. D. Axelrod, in *Spectroscopy and the Dynamics of Molecular Biological Systems*, eds. P. M. Bayley and R. E. Dale (Academic Press, London, 1985), pp. 163–176.
52. N. O. Petersen, S. Felder and E. L. Elson, in *Handbook of Experimental Immunology*, Vol. 1, eds. D. M. Weir, C. Blackwell and L. A. Herzenberg (Blackwell Science Publishers, Palo Alto, 1986), pp. 24.1–24.23.
53. M. P. Sheetz, S. Turney, H. Qian and E. L. Elson, Nature **340**, 284 (1989).
54. D. F. Kucik, E. L. Elson and M. P. Sheetz, Nature **340**, 315 (1989).
55. D. Haft and M. Edidin, Nature **340**, 262 (1989).
56. M. de Brabander, R. Nuydens, A. Ishihara, B. Holifield, K. Jacobson and H. Geerts, J. Cell Biol., in press (1990).
57. R. N. Ghosh and W. W. Webb, Biophys. J. **57**, 286a (Abstract) (1990).
58. G. M. Lee, A. Ishihara and K. A. Jacobson, J. Cell Biol. **111**, 72a (Abstract) (1990).
59. R. D. Tilton, A. P. Gast and C. R. Robertson, Biophys. J. **58**, 1321 (1990).
60. S. Subramaniam, M. Seul and H. M. McConnell, Proc. Natl. Acad. Sci. USA **83**, 1169 (1986).
61. L. K. Tamm, Biochemistry **27**, 1450 (1988).
62. L. L. Wright, A. G. Palmer III and N. L. Thompson, Biophys. J. **54**, 463 (1988).
63. N. L. Thompson, A. A. Brian and H. M. McConnell, Biochim. Biophys. Acta **772**, 10 (1984).
64. D. W. Tank, E. S. Wu, P. R. Meers and W. W. Webb, Biophys. J. **40**, 129 (1982).
65. R. Peters and R. J. Cherry, Proc. Natl. Acad. Sci. USA **79**, 4317 (1982).
66. L. T. Pearson, S. I. Chan, B. A. Lewis and D. M. Engelman, Biophys. J. **43**, 167 (1983).
67. B. Chazotte and C. R. Hackenbrock, J. Biol. Chem. **263**, 14359 (1988).
68. J. Braun, J. R. Abney and J. C. Owicki, Nature **310**, 316 (1984).
69. J. R. Abney, J. Braun and J. C. Owicki, Biophys. J. **52**, 441 (1987).
70. M. J. Saxton, Biophys. J. **39**, 165 (1982).
71. T. J. O'Leary, Proc. Natl. Acad. Sci. USA **84**, 429 (1987).
72. D. Stauffer, *Introduction to Percolation Theory* (Taylor & Francis, London, 1985).
73. J. Feder, *Fractals* (Plenum Press, New York, 1988).
74. V. A. Petit and M. Edidin, Science **184**, 1183 (1974).
75. T. Ohtsuki, Physica **122A**, 212 (1983).
76. H. Berg, *Random Walks in Biology* (Princeton University Press, Princeton, New Jersey, 1983).
77. D. A. McQuarrie, *Statistical Mechanics* (Harper and Row, New York, 1976).
78. H. Van Beijeren and R. Kutner, Phys. Rev. Lett. **55**, 238 (1985).
79. N. J. Wagner and W. B. Russel, Physica A **155**, 475 (1989).
80. R. K. Small, M. Blank, R. Ghez and K. H. Pfenninger, J. Cell Biol. **98**, 1434 (1984).
81. M. F. Blackwell and J. Whitmarsh, Biophys. J. **58**, 1259 (1990).
82. J. Braun, J. R. Abney and J. C. Owicki, Biophys. J. **52**, 427 (1987).
83. W. H. Press, B. P. Flannery, S. A. Teukolsky and W. T. Vetterling, *Numerical Recipes: The Art of Scientific Computing* (Cambridge University Press, Cambridge, 1986).